Disease-specific molecular events in cortical multiple sclerosis lesions

doi:10.1093/brain/awt110 Brain 2013: 136; 1799–1815 | 1799

BRAIN
A JOURNAL OF NEUROLOGY

Disease-specific molecular events in cortical multiple sclerosis lesions

Marie Therese Fischer,[1,*] Isabella Wimmer,[1,*] Romana Höftberger,[2] Susanna Gerlach,[1] Lukas Haider,[1] Tobias Zrzavy,[1] Simon Hametner,[1] Don Mahad,[3] Christoph J. Binder,[4] Markus Krumbholz,[5] Jan Bauer,[1] Monika Bradl[1] and Hans Lassmann[1]

1 Department of Neuroimmunology, Centre for Brain Research, Medical University of Vienna, Austria
2 Institute of Neurology, Medical University of Vienna, Austria
3 The Mitochondrial Research Group, Institute for Ageing and Health, Newcastle University, Framlington Place, Newcastle upon Tyne, NE2 4HH, UK
4 Research Centre for Molecular Medicine (CeMM) of the Austrian Academy of Sciences and Department of Laboratory Medicine, Medical University of Vienna, Austria
5 Institute of Clinical Neuroimmunology, Ludwig Maximilian University Munich, Germany

*These authors contributed equally to this work.

Correspondence to: Prof. Dr. Hans Lassmann,
Centre for Brain Research,
Medical University of Vienna,
Spitalgasse 4,
A-1090 Wien
E-mail: hans.lassmann@meduniwien.ac.at

Cortical lesions constitute an important part of multiple sclerosis pathology. Although inflammation appears to play a role in their formation, the mechanisms leading to demyelination and neurodegeneration are poorly understood. We aimed to identify some of these mechanisms by combining gene expression studies with neuropathological analysis. In our study, we showed that the combination of inflammation, plaque-like primary demyelination and neurodegeneration in the cortex is specific for multiple sclerosis and is not seen in other chronic inflammatory diseases mediated by CD8-positive T cells (Rasmussen's encephalitis), B cells (B cell lymphoma) or complex chronic inflammation (tuberculous meningitis, luetic meningitis or chronic purulent meningitis). In addition, we performed genome-wide microarray analysis comparing micro-dissected active cortical multiple sclerosis lesions with those of tuberculous meningitis (inflammatory control), Alzheimer's disease (neurodegenerative control) and with cortices of age-matched controls. More than 80% of the identified multiple sclerosis-specific genes were related to T cell-mediated inflammation, microglia activation, oxidative injury, DNA damage and repair, remyelination and regenerative processes. Finally, we confirmed by immunohistochemistry that oxidative damage in cortical multiple sclerosis lesions is associated with oligodendrocyte and neuronal injury, the latter also affecting axons and dendrites. Our study provides new insights into the complex mechanisms of neurodegeneration and regeneration in the cortex of patients with multiple sclerosis.

Keywords: multiple sclerosis; cortex; gene expression; demyelination; neurodegeneration
Abbreviation: PLP = proteolipid protein; TUNEL = terminal deoxynucleotidyl transferase dUTP nick end labelling

Received October 16, 2012. Revised March 5, 2013. Accepted March 23, 2013. Advance Access publication May 17, 2013

Introduction

Multiple sclerosis is traditionally seen as a disease that affects the white matter giving rise to focal inflammatory demyelinating lesions (Lassmann *et al*., 2007). Recent studies on the pathology of multiple sclerosis, however, challenged this concept by providing evidence for extensive grey matter lesions in the cerebral (Peterson *et al*., 2001; Bo *et al*., 2003; Kutzelnigg *et al*., 2005) and cerebellar cortex (Kutzelnigg *et al*., 2007) and in the hippocampus (Geurts *et al*., 2007). Despite the primary demyelinating nature of cortical lesions, profound degeneration also affects cortical neurons, axons and synapses (Peterson *et al*., 2001; Wegner *et al*., 2006; Dutta and Trapp, 2011).

Cortical lesions arising during early (Lucchinetti *et al*., 2011) and late (Kutzelnigg *et al*., 2005; Howell *et al*., 2011) disease stages are associated with inflammation. In lesions developing in the progressive stage, the degree of meningeal inflammation correlates with the extent of active demyelination and neurodegeneration (Howell *et al*., 2011; Choi *et al*., 2012). Thus, inflammation may drive cortical lesions, but it remains unresolved, whether cortical primary demyelination is a multiple sclerosis-specific event, which types of inflammatory cells are involved and which molecular mechanisms evoke tissue injury. In this study, we compared cortical pathology in multiple sclerosis with that seen in a large spectrum of other inflammatory and neurodegenerative brain diseases and found that the combination of inflammation, plaque-like primary demyelination and neurodegeneration is specific for multiple sclerosis. The second part of the study focused on global gene expression studies analysing potential molecular pathways of tissue injury in active cortical multiple sclerosis lesions. The latter were defined by the presence of macrophages containing degradation products reactive for myelin or neuronal antigens. Since the data suggested oxidative injury, DNA damage, and apoptosis as potential mechanisms of tissue degeneration, we analysed the expression of proteins involved in oxidative burst as well as the presence of oxidized lipids and DNA fragmentation in a broad sample of cortical multiple sclerosis lesions in comparison with the normal and diseased controls using immunohistochemistry and terminal deoxynucleotidyl transferase dUTP nick end labelling (TUNEL) staining.

Materials and methods

Sample characterization

Archival formaldehyde-fixed and paraffin-embedded (FFPE) autopsy material collected in the archives of the Centre for Brain Research and the Institute of Neurology were used (Table 1). The study was approved by the Ethical Committee of the Medical University of Vienna (EK. No. 535/2004 and 087/01/2012). It included 21 cases of multiple sclerosis comprising acute multiple sclerosis ($n = 6$), relapsing-remitting multiple sclerosis ($n = 1$), secondary progressive multiple sclerosis ($n = 7$) and primary progressive multiple sclerosis ($n = 7$). As controls, cases of chronic tuberculous meningitis ($n = 4$), luetic meningitis ($n = 1$), chronic purulent meningitis ($n = 1$), Rasmussen's encephalitis ($n = 5$), B cell lymphomas affecting meninges and cortex (including one EBV$^+$ lymphoma; $n = 4$), Alzheimer's disease ($n = 11$) and age-matched controls without any detectable brain disease (control subjects; $n = 17$) were included. For basic neuropathology of each case, multiple tissue blocks from all brain regions were stained with haematoxylin/eosin, Luxol Fast blue myelin stain and Bielschowsky silver impregnation. The selection of tissue blocks taken for microarray and neuropathological analysis depended on the clinical diagnosis of each patient (Table 1). For microarray analysis we selected frontal association cortex for multiple sclerosis and controls, frontobasal (TB1 and TB2) and temporobasal (TB3) cortex for tuberculous meningitis and temporal cortex for Alzheimer's disease. For neuropathological studies the blocks (between three and eight) from patients with Alzheimer's disease or tuberculous meningitis included cortical areas (frontal, temporal, parietal and occipital), while in case of B cell lymphoma between one and three blocks were chosen, which contained infiltration of neoplastic B cells in meninges or cortex (frontal and parietal). Tissue samples from patients with Rasmussen's encephalitis derived from temporal cortico/subcortical neurosurgical resections and were, thus, restricted to one block per case. For control cases, basic neuropathology was performed on eight to 15 tissue blocks from all brain regions to exclude confounding pathology. From those three to six blocks comprising frontal, parietal, and temporal cortex were selected for further analysis. In multiple sclerosis cases, cortical lesions were either identified by analysis of multiple tissue blocks ($n = 10$ cases) or were specifically trimmed from hemispheric or double hemispheric sections ($n = 11$ cases). The architecture of active cortical lesions was complex. In general, they contained a fully demyelinated area, which was surrounded by an area of variable size with reduced myelin density and profound microglia activation, located between the demyelinated lesion and the normal appearing grey matter. However, microglia activation alone was not sufficient for the identification of an active lesion, since a rim of activated (iron containing) microglia can be seen in multiple sclerosis lesions, which do not expand in the subsequent years (Bian *et al*., 2012). Thus, we used the presence of degradation products in macrophages reactive for myelin or neuronal antigens, such as neurofilament, as an additional marker for active cortical lesions (Fig. 1 and Supplementary Fig. 1). For the investigation of molecular mechanisms of tissue injury by microarray analysis, we selected subpial cortical lesions with a zone of perilesional activity as defined above.

Immunohistochemistry

Consecutive 5-µm thick serial sections were cut, routinely deparaffinized and endogenous peroxidase was blocked with H_2O_2/methanol. Non-specific antibody binding was blocked by incubating the section in 10% foetal calf serum. Antigen retrieval procedures and primary antibodies used for immunohistochemistry are listed in Table 2. Primary antibodies were applied overnight at 4°C. For immunohistochemical controls, either primary antibodies were omitted or unrelated sera or monoclonal antibodies of the same immunoglobulin class were used. Antibody binding was routinely visualized using 3,3′-diaminobenzidine, which was occasionally enhanced by biotinylated tyramine amplification (King *et al*., 1997). Alternatively, Fast blue B salt or 3-amino-9-ethylcarbazole were used for signal development. Before mounting of sections, cell nuclei were counterstained with haematoxylin.

Confocal fluorescence immunohistochemistry was performed on paraffin sections as described for light microscopy with some modifications. For fluorescent double labelling with primary antibodies from different species (mouse-anti-E06 and goat-anti-carbonic anhydrase II, rabbit-anti-GFAP, rabbit-anti-neurofilament or rabbit-anti-calbindin,

Table 1 Clinical demographics

Case ID	Details	Age	Sex	Disease duration	Progressive phase duration	Total number of tissue blocks	Block types
MS1*	**SPMS**	**42**	**F**	**216 months**	**168 months**	**6**	**C**
MS2*	**SPMS**	**41**	**M**	**137 months**	**n.a.**	**34**	**A, C**
MS3*	**SPMS**	**46**	**F**	**444 months**	**228 months**	**21**	**A, C**
MS4	AMS	34	F	4 months	0	1	B
MS5	AMS	35	M	1.5 months	0	11	A, C
MS6	AMS	45	M	0.2 months	0	3	B
MS7	AMS	45	M	0.6 months	0	3	B, C
MS8	AMS	52	M	1.5 months	0	3	C
MS9	AMS	78	M	2 months	0	14	C
MS10	RRMS	57	F	156 months	0	13	B, C
MS11	SPMS	66	F	96 months	n.a.	39	C
MS12	SPMS	34	M	120 months	n.a.	16	C
MS13	SPMS	53	F	241 months	104 months	23	A, C
MS14	SPMS	56	M	372 months	126 months	46	A, C
MS15	PPMS	55	F	60 months	60 months	10	A, C
MS16	PPMS	54	F	72 months	72 months	12	C
MS17	PPMS	67	M	87 months	87 months	41	A, C
MS18	PPMS	77	F	168 months	168 months	11	C
MS19	PPMS	53	M	168 months	168 months	16	C
MS20	PPMS	34	M	204 months	204 months	7	C
MS21	PPMS	71	F	264 months	264 months	9	C
TB1*		**67**	**F**	**1 month**		**15**	**C**
TB2*		**48**	**M**	**n.a.**		**6**	**C**
TB3*		**24**	**F**	**2 weeks**		**4**	**C**
TB4		19	M	1 month		8	C
LU1		58	F	n.a.		2	C
ME1		62	M	8 days		1	C
BLY1		59	F	n.a.		3	C
BLY2		63	F	3 weeks		10	C
BLY3		71	M	11 months		11	C
BLY4	EBV+	47	M	1.5 months		22	C
RAE1		3.9	F	17 months		1	D
RAE2		15	F	7.5 months		1	D
RAE3		22	M	7.1 months		1	D
RAE4		24	M	58 months		1	D
RAE5		28	F	27 months		1	D
AD1*	**Braak VI**	**89**	**F**	**36 months**		**8**	**C**
AD2*	**Braak VI**	**82**	**F**	**90 months**		**5**	**C**
AD3*	**Braak VI**	**60**	**F**	**72 months**		**24**	**C**
AD4	Braak III	66	F	n.a.		22	C
AD5	Braak V	70	F	96 months		8	C
AD6	Braak IV	79	F	60 months		10	C
AD7	Braak IV	81	F	36 months		23	C
AD8	Braak V	86	F	60 months		7	C
AD9	Braak VI	86	F	n.a.		8	C
AD10	Braak VI	86	F	n.a.		10	C
AD11	Braak IV	92	F	n.a.		7	C
CO1*		**45**	**F**	**0**		**5**	**C**
CO2*		**46**	**M**	**0**		**3**	**C**
CO3*		**65**	**M**	**0**		**4**	**C**
CO4		30	F	0		3	C
CO5		36	F	0		3	C
CO6		39	F	0		3	C
CO7		37	M	0		4	C
CO8		42	F	0		3	C
CO9		47	F	0		3	C
CO10		70	M	0		3	C
CO11		71	F	0		3	C
CO12		71	F	0		3	C
CO13		72	M	0		3	C
CO14		83	M	0		6	C
CO15		84	F	0		3	C
CO16		88	F	0		3	C
CO17		97	F	0		3	C

MS = multiple sclerosis; AMS = acute MS; RRMS = relapsing remitting MS; PPMS = primary progressive multiple sclerosis; SPMS = secondary progressive multiple sclerosis; TB = tuberculous meningitis; LU = luetic meningitis; ME = chronic purulent meningitis; BLY = B-cell lymphoma; RAE = Rasmussen's encephalitis; AD = Alzheimer's disease; Braak = Braak stages of Alzheimer's disease; CO = control without neurological disease or brain lesions; f = female; m = male; n.a. = data not available; * = case included in microarray study printed in bold; Block types: A = double hemispheric blocks; B = single hemispheric blocks; C = conventional blocks (2 × 3 cm).

respectively), antibodies were applied simultaneously at 4°C overnight. After washing, secondary antibodies (biotin-conjugated donkey-anti-rabbit, 1:200; Cy3-conjugated donkey-anti-goat, 1:200; Cy2-conjugated donkey-anti-mouse, 1:200; all antibodies from Jackson ImmunoResearch) were applied simultaneously for 1 h at room temperature. This procedure was followed by application of streptavidin-Cy5 (Jackson ImmunoResearch; 1:75) for 1 h at room temperature. Finally, fluorescent preparations were embedded and examined using a confocal laser scan microscope (Leica SP5) equipped with lasers for 488, 543 and 633 nm excitation. Scanning for Cy2 (488 nm), Cy3 (543 nm) and Cy5 (633 nm) was done sequentially to rule out fluorescence bleed through.

TUNEL staining for DNA damage

TUNEL staining was performed essentially as described previously (Gold *et al*., 1993) and has already successfully been applied previously for analysis of DNA fragmentation in Alzheimer's disease and controls (Lassmann *et al*., 1995). In the present study we used the *In Situ* Cell Death Detection Kit (Roche).

Quantification of immunohistochemistry and TUNEL staining

CD3-positive T cells, CD68-positive macrophages, TPPP/p25-positive oligodendrocytes, neurofilament-reactive dystrophic axons, neuronal cell bodies, E06-positive neurons and TUNEL-positive cells were counted. In case of neuronal quantification, only neurons containing a nucleus with a prominent nucleolus were included. Counting of neurons, oligodendrocytes, dystrophic axons and TUNEL-positive cells was performed in cortical layers III to V. Quantitative analysis was done using a morphometric grid within the ocular lens counting 10 microscopic fields of 0.0576 mm^2 per region of interest (normal appearing grey matter and lesion). Presented values were calculated as counts/mm^2 tissue area. Quantitative enumeration of T cells and macrophages was done in the entire cortex, including the meninges, positioning the grid areas in parallel rows, spanning the entire cortical ribbon. The percentage of neurons with intense cytoplasmic reactivity for oxidized phospholipids (E06 reactivity) is shown in relation to the

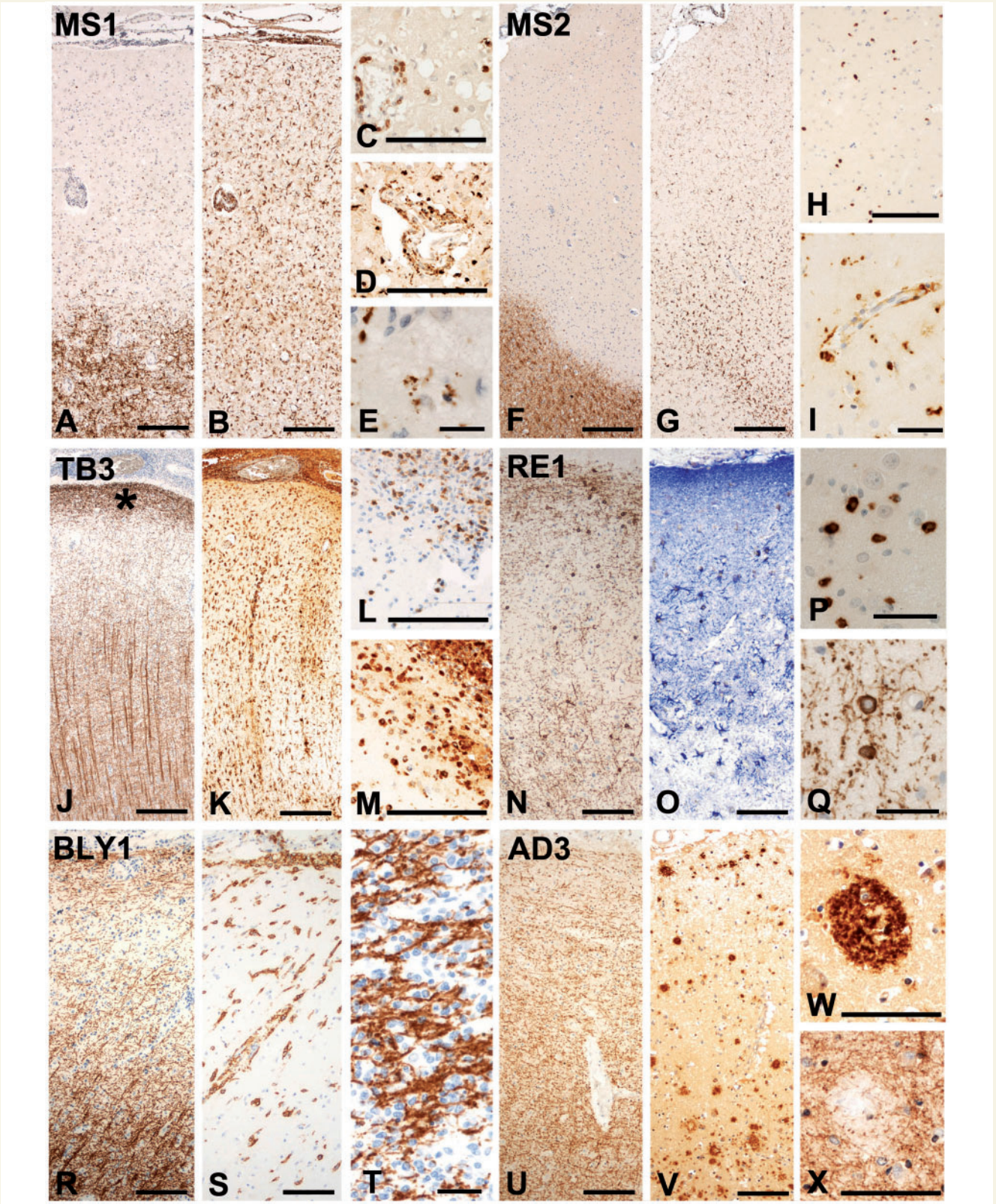

Figure 1 Plaque-like primary demyelination is specific for multiple sclerosis. (**A–E**) Highly inflammatory, active cortical lesion from Case MS1. Extensive subpial demyelination [**A**; immunohistochemistry (IHC) for PLP] is associated with inflammatory infiltrates in the meninges and the perivascular space. Profound activation of microglia is visible in the lesion and in the adjacent periplaque grey matter (**B**; IHC for HLA-D). CD3-positive T lymphocytes are present in the perivascular inflammatory cuffs and diffusely dispersed throughout the lesion (**C**; IHC for CD3). Phagocytic macrophages are also present in the perivascular inflammatory cuffs and in the parenchyma (**D**; IHC for CD68). They in part contain myelin degradation products reactive for PLP (**E**; IHC for PLP). (**F-I**) Chronic, active cortical lesion from

(continued)

total number of counted cortical neurons. To examine the extent of demyelination, proteolipid protein (PLP)-stained slides were scanned and the extent of demyelination was calculated as demyelinated area in relation to total cortex area.

RNA extraction and microarrays

For gene expression studies, three active multiple sclerosis lesions (the fulminate active lesion of Case MS1 and two chronic active lesions from Cases MS2 and MS3), three cortex samples from patients with tuberculous meningitis, three Alzheimer's disease cases, and three controls without brain pathology were selected (Table 1).

As archival formaldehyde-fixed and paraffin-embedded autopsy material with unknown time spans and storage conditions between sampling and fixation was used, RNA preservation of more than 150 multiple sclerosis tissue blocks and 40 tissue blocks containing control material (Alzheimer's disease, tuberculous meningitis, control subjects), was assessed by *in situ* hybridization for PLP as described (Breitschopf *et al*., 1992). Tissue blocks with strong and specific *in situ* hybridization signals in oligodendrocytes after short development time (<10 h) were selected for further studies. Ten to 20 6–10-µm thick sections were cut under RNase-free conditions. Cortical tissue blocks for microarray analysis were selected according to the presence of lesions typical for the different disease entities. Cortical areas including all cortical layers from Alzheimer's disease, tuberculous meningitis and control subjects were micro-dissected. In tuberculous meningitis cases, these cortical areas were further restricted to sites with profound meningeal and parenchymal inflammation. For multiple sclerosis cases, we microdissected cortical areas with subpial demyelination of at least the outer four cortical layers. These lesions contained a broad zone around the plaque with profound microglia activation and the presence of macrophages with degradation products reactive for myelin or neuronal antigens. Thus, for messenger RNA analysis, these multiple sclerosis blocks also contained all cortical layers and, dependent on the degree of activity, a zone of variable size with signs of active tissue injury. Isolation, amplification, and quality assessment of messenger RNA were done as extensively described before (Fischer *et al*., 2012). Briefly, total RNA was isolated using the High Pure FFPE RNA Micro Kit (Roche) according to the manufacturer's instructions. The concentration of isolated total RNA was too low for any RNA integrity measurements. Instead, messenger RNA was amplified using poly(T) primers and the Arcturus® Paradise® FFPE Amplification Kit (Applied Biosystems, Life Technology). After the first round of *in vitro* transcription, the quality of the samples was tested. Owing to RNA fragmentation and cross-linking during formaldehyde fixation, it is almost impossible to isolate full length RNA from formaldehyde-fixed and paraffin-embedded tissue. Therefore, routine endpoint PCR for the housekeeping gene actin, beta (*ACTB*) was performed to verify that RNA fragments were sufficiently long to use them as probes for microarrays. Primers were designed in such a way that the forward primer binds 472 bases upstream of the poly(A) tail. Endpoint PCR was run with the following settings: forward: 5′-TTGACTCAGGATTTAAAA ACTGG-3′, reverse: 5′-AGGGACTTCCTGTAACAACGC-3′; 10 min denaturation; followed by 40 cycles of denaturation (30 s, 95°C), annealing (30 s, 55°C), and extension (30 s, 72°C). Only when a sufficient amount of PCR product was found, the samples qualified for a second round of *in vitro* amplification. The resulting antisense RNA was sent out for hybridization to Agilent-014850 Whole-Human Genome Microarrays 4x44K (G4112F). RNA labelling, microarray hybridization and scanning, as well as quantile normalization of raw data were carried out externally (Source BioScience imaGenes GmbH).

For data analysis, two different approaches were used. On the one hand, all genes significantly changed ($P < 0.01$; Student's *t*-test) in cases with multiple sclerosis (Cases MS1–3) in comparison with other cases (Alzheimer's disease, tuberculous meningitis and control subjects) were evaluated. On the other hand, to have the ability to assess the inflammatory component of the fulminate lesion of Case MS1, all massively up- or down regulated genes ($\log_2$ fold-changes >4 or <-4.5, respectively) in Case MS1 in comparison with all other cases (other multiple sclerosis, Alzheimer's disease, tuberculous meningitis and control subjects) were examined. As significance testing was not possible for this analysis approach, restrictive cut-offs were used instead. They were based on the observation that above and below a $\log_2$ fold-change of 4 and 4.5, respectively, the detected differences were granted to be exclusively present in Case MS1, whereas the gene expression values in all other cases (tuberculous meningitis, Alzheimer's disease and control subjects) were low. Functions of the multiple sclerosis-specific genes were determined based on several sources: PhosphoSitePlus® (http://www.phosphosite.org), NCBI (http://www.ncbi.nlm.nih.gov/), Panther classification system (http://www.

Figure 1 Continued

Case MS2. Subpial demyelination (**F**; IHC for PLP) and inflammation in the meninges are seen. The active edge of the lesion is characterized by dense microglia and macrophage infiltration (**G**; IHC for Iba-1). In the active area with high microglia density, there is also a diffuse infiltration of CD3-positive T cells into the cortical parenchyma (**H**; IHC for CD3). Phagocytic macrophages are present and concentrated at the lesion edge (**I**; IHC for CD68). (**J**-**M**) Cortical lesions in tuberculous meningitis (Case TB3). There is profound inflammation in the meninges and extensive microglia activation throughout the whole cortex (**K**; IHC for HLA-D), but cortical myelin architecture is preserved showing a broad band of myelinated fibres at the subpial surface (indicated by an asterisk in **J**), low myelin content in layers 2 and 3 and much higher myelin content in the deeper cortical layers (**J**; IHC for MBP). In the superficial cortical areas, which show normal myelin content, there is an extensive tissue infiltration by T cells (**L**; IHC for CD3) and phagocytic macrophages (**M**; IHC for CD68). (**N**-**Q**) Cortical lesion from a patient with Rasmussen's encephalitis (RE1). Despite extensive cortical infiltration by CD8-positive T cells (**P**; IHC for CD8), neuronal loss (Bien *et al*., 2002) and patchy loss of astrocytes (Bauer *et al*., 2007) (**O**: IHC for GFAP), myelin and oligodendrocytes are not affected (**N**, **Q**; IHC for CNPase). (**R**-**T**) Cortical lesion from a patient with B cell lymphoma (BLY1). There is profound meningeal, perivascular and parenchymal infiltration by neoplastic B cells (**S**; IHC for CD20), but the myelin architecture of the cortex is preserved (**R**; IHC for MBP). In areas of very dense neoplastic B cell infiltration, myelin is pushed aside by aggregated B cells, but there is no indication of demyelination (**T**; IHC for MBP). (**U**-**X**) Cortical lesion from a patient with Alzheimer's disease (AD3). There are numerous amyloid plaques in the cortex (**V**; IHC for Aß peptide), but the architecture of cortical myelin is preserved (**U**; IHC for PLP). Only in the centre of amyloid plaques (**W**; IHC for Aß), there is a minor loss of myelin (**X**; IHC for PLP). MS = multiple sclerosis; TB = tuberculous meningitis; RE = Rasmussen's encephalitis; BLY = B cell lymphoma; AD = Alzheimer's disease; *subpial myelin band. Scale bar = 100 µm for **A–D**, **F–H**, **J**-**O**, **R**, **S** and **U–X**; Scale bar = 50 µm **for E**, **I**, **P**, **Q** and **T**.

Table 2 Antigen retrieval and primary antibodies

Antibody	Origin	Target	Dilution	Antigen retrieval	Source
Aß	Mouse (mAB)	Aß peptide	1:500	St (FA or E)	MAB1516; Chemicon
AIF	Rabbit (pAB)	Apoptosis inducing factor	1:250	St (C)	AB16501; Chemicon
APP	Mouse (mAB)	Amyloid precursor protein	1:1000	St (C)	MAB348; Chemicon
AQP1	Rabbit (pAB)	Aquaporin 1	1:500	0	sc-20810; Santa Cruz Biotechnoloy
C9neo	Rabbit (pAB)	Complement component C9	1:2000	P, #	Piddlesden *et al*., 1993
CA II	Sheep (pAB)	Carbonic anhydrase II	1:1000	St (E)	PC076; The Binding Site
Caspase 3	Rabbit (pAB)	Activated caspase 3	1:10000	St (C)	551150; BD Biosciences
CB	Rabbit (pAB)	Calbindin	1:500	St (C)	CB-38; SWant Swiss Antibodies
CD3	Rabbit (mAB)	T-cells	1:2000	St (E), *	RM-9107-S; Neomarkers
CD8	Mouse (mAB)	MHC Class I restricted T-cells	1:250	St (E), *	M7103; Dako
CD20	Mouse (mAB)	B-cells	1:100	St (E)	MS-340-S; Neomarkers
CD68	Mouse (mAB)	Phagocytic macrophages	1:100	St (E)	M0814; Dako
CD163	Mouse (mAB)	Macrophage scavenger receptor	1:1000	St (C), *	NCL-CD163; Novocastra
CNPase	Mouse (mAB)	2′,3′-Cyclic nucleotide 3′ phosphodiesterase	1:2000	St (E)	SMI 91; Sternberger Monoclonals
E06	Mouse (mAB)	Oxidized phospholipids	10 µ/ml	0 or St (C or E)	Palinski *et al*., 1996
GFAP	Rabbit (pAB)	Glial fibrillary acidic protein	1:3000	St (E), +	Z0334; Dako
Granzyme B	Mouse (mAB)	Granzyme B	1:1000	St (E), *	MS-1157-S; Neomarkers
HC10	Mouse (mAB)	MHC I heavy chain	1:2000	St (E), *	Stam *et al*., 1990
HLA-D	Mouse (mAB)	Human leucocyte antigen (DP, DQ, DR)	1:100	St (C)	M0775; Dako
IBA-1	Rabbit (pAB)	Ionized calcium binding adaptor molecule 1	1:3000	St (E)	019-19741; WAKO Chemicals
Ig	Sheep (pAB)	Human immunoglobulin	1:200	P	RPM1003; Amersham Pharmacia Biotech
iNOS	Rabbit (pAB)	Inducible nitric oxide synthase	1:30000	St (E), +	AB5384; Chemicon
MBP	Rabbit (pAB)	Myelin basic protein	1:2500	0	A0623; Dako
NF	Rabbit (pAB)	Neurofilament medium chain (150 kDa)	1:2000	St (E)	AB1981; Chemicon
P22phox	Rabbit (pAB)	NADPH oxidase protein	1:100	St (C), +	sc-20781; Santa Cruz Biotechnology
PECAM-1	Mouse (mAB)	Platelet/endothelial cell adhesion molecule-1	1:250	St (E)	MS-353; NeoMarkers
PLP	Mouse (mAB)	Proteolipid protein	1:1000	St (E)	MCA839G; Serotec
SY	Rabbit (mAB)	Synaptophysin	1:100	St (C)	1485-1; Epitomics
TPPP/p25	Rat (pAB)	Tubulin polymerization promoting protein	1:3000	St (E)	Hoftberger *et al*., 2010

0 = no antigen retrieval; St = steaming of sections using the indicated buffer solution; C = citrate buffer (pH 6.0); E = EDTA buffer (pH 9.0); P = protease predigestion; FA = formic acid; mAB = monoclonal antibody; pAB = polyclonal antibody; * = 3,3′-diaminobenzidine development enhanced by biotinylated tyramine amplification (King *et al*., 1997); # = antibody labelling visualized with 3-amino-9-ethylcarbazole instead of routinely used 3,3′-diaminobenzidine; + = antibody labelling visualized with Fast blue B instead of routinely used 3,3′-diaminobenzidine.

pantherdb.org), and KEGG Kyoto Encyclopaedia of Genes and Genomes (http://www.genome.jp/kegg). Particularly, PubMed was screened for genes with known functions in multiple sclerosis or experimental autoimmune encephalomyelitis.

Based on the microarray data (deposited in NCBI's Gene Expression Omnibus; GEO Accession Number GSE32645), genes related to inflammation, structural changes, or oxidative injury were selected and immunohistochemistry was performed on serial sections immediately adjacent to the sections used for gene expression profiling. For these exemplary genes, it could be shown that protein expression visualized by immunohistochemistry followed the up- and down regulation trends of the microarray data (Supplementary Fig. 1). Furthermore, TaqMan® real-time PCR was performed to validate selected multiple sclerosis-specific genes (Supplementary Table 4).

Statistical analysis

Descriptive analysis included median value and range, percentages, scatter plots and box plots. For comparisons of multiple groups, the Kruskal-Wallis test was used, followed by pair-wise Mann-Whitney U-tests and Bonferroni-Holm correction. For the analysis of microarray data (Cases MS1–3 in comparison with all other cases pooled in one group), Student's *t*-tests were performed. The reported *P*-values are results of two-sided tests. A *P*-value $\leqslant 0.05$ was considered statistically significant. Analyses were done using PASW Statistics 18 (SPSS Inc.).

Results

Focal lesions of primary demyelination are specific for multiple sclerosis

In a first step, we analysed demyelination and neurodegeneration in the cortex of patients with multiple sclerosis in comparison with other inflammatory and neurodegenerative diseases. In multiple sclerosis, cortical pathology was characterized by the presence of

large plaques of primary demyelination (complete loss of myelin with axonal preservation such as preservation of phosphorylated neurofilament-reactive profiles) as described previously (Peterson *et al*., 2001; Kutzelnigg *et al*., 2005). In one case of secondary progressive multiple sclerosis (Case MS1), fulminate inflammatory cortical lesions were present, similar to those described in early multiple sclerosis (Lucchinetti *et al*., 2011) with profound inflammation in the meninges (Fig. 1B), abundant perivascular inflammatory cuffs (Fig. 1D and Supplementary Fig. 1) and T and B lymphocyte infiltration into the cortical parenchyma (Fig. 1C and Supplementary Table 1). Active cortical demyelination (Fig. 1A) was reflected by the presence of activated macrophages containing myelin degradation products reactive for PLP (Fig. 1E). The other multiple sclerosis cases (shown representatively by Case MS2 in Fig. 1F–I) exhibited cortical demyelinated lesions as described (Howell *et al*., 2011). In these expanding cortical lesions, lymphocyte infiltration was restricted to the meninges and the zones of lesional activity. A variable degree of microglia activation was observed, forming a band of high cell density at the margin towards the normal appearing grey matter (see Supplementary Fig. 1). In these areas, few diffusely dispersed T cells were present (Fig. 1H) and microglia cells contained myelin degradation products.

Cortical lesions in patients with tuberculous or luetic meningitis also showed strong meningeal and parenchymal inflammation with a similar cellular composition of T cells, B cells, plasma cells, and macrophages as in multiple sclerosis (Fig. 1K–M). In some cases, the infiltrates additionally contained granulocytes. Despite the massive inflammatory reaction in the cortex, no focal primary plaque-like demyelination was present (Fig. 1J).

Cortical lesions from patients with Rasmussen's encephalitis (a paradigmatic example of encephalitis mediated by MHC class I restricted T cells) showed only minor meningeal inflammation, dominated by T cells and macrophages, but profound diffuse T cell infiltration of the cortical parenchyma (Fig. 1P). These infiltrates were associated with massive microglia activation and neuronal and astrocytic degeneration (Fig. 1O) (Bien *et al*., 2002; Bauer *et al*., 2007). Again, no indication for focal multiple sclerosis-like primary demyelination was found (Fig. 1N and Q).

In B cell lymphomas affecting the cortex, massive infiltration of the meninges and the cortical parenchyma by neoplastic B cells (Fig. 1S) and a variable extent of T cell infiltration and microglia activation were seen. In severely affected regions, this resulted in displacement of the cortical parenchyma by neoplastic cells. In areas of very dense B cell infiltration, myelin was pushed aside by aggregated B lymphocytes (Fig. 1T), but there was no indication of primary demyelination (Fig. 1R).

No plaque-like demyelination was present in the cortex of patients with Alzheimer's disease (Fig. 1U). However, immunohistochemistry for proteolipid protein revealed a minor loss of myelin within the core and the vicinity of amyloid plaques (Fig. 1V–X) (Mitew *et al*., 2010).

These data indicate that the formation of plaque-like primary demyelinating cortical lesions is multiple sclerosis-specific and does not simply reflect tissue damage induced by inflammatory mechanisms or mediators.

Comparative analysis of gene expression in cortical lesions

Quantitative immunohistochemistry (Table 3) of disease and control cases selected for our microarray study confirmed that inflammation mediated by T cells, B cells, and microglia activation were most pronounced in tuberculous meningitis, whereas demyelination and oligodendrocyte loss were restricted to multiple sclerosis lesions. Neuronal and axonal injury was present in multiple sclerosis, tuberculous meningitis, and Alzheimer's disease, but was highest in multiple sclerosis compared with the other diseases.

Analysing our microarray data, we found 109 genes significantly up- or downregulated in multiple sclerosis in comparison with all other disease and control cases ($P < 0.01$; Supplementary Table 2). In a separate approach, we examined gene expression in Case MS1, which presented with fulminate inflammatory cortical demyelination. Comparing this single multiple sclerosis case with all other cases included in our gene expression study allowed us to specifically examine the inflammatory component of this active cortical lesion. As a restrictive cut-off point we chose genes that were differentially up- (>4-fold $\log_2$) or downregulated (<-4.5-fold $\log_2$) compared with all other cases, including tuberculous meningitis cases showing the highest extent of inflammation. This resulted in 192 hits (144 upregulated and 48 downregulated; Supplementary Table 3). Taking together the two analysis approaches, we identified 301 multiple sclerosis-specific genes. Among those genes, 82% could be grouped into three major categories (Fig. 2 and Supplementary Tables 2 and 3): inflammation and immune cell activation/migration (24%), oxidative injury, DNA damage/repair, and cell death (28%), and tissue repair/regeneration (52%). Assignment of genes to multiple categories was tolerated. A comprehensive tabular summary of all multiple sclerosis-specific genes including $\log_2$ fold-changes, *P*-values, gene accessions and gene functions, can be found in Supplementary Tables 2 and 3.

Category 1: genes associated with inflammation

Differential expression of inflammation-associated genes was mainly seen in the highly inflammatory cortical lesions of Case MS1 (Supplementary Table 3). Functional grouping revealed that many of the identified genes code for proteins involved in antigen recognition of class I and class II restricted T cells and in the regulation of Th1 and Th17 T-cell responses (10 genes), in microglia and macrophage function (seven genes), and in chemokine/cytokine signalling and leucocyte recruitment (18 genes). Profound multiple sclerosis-specific changes were also seen for genes involved in synthesis and function of selectins.

Category 2: genes associated with cell death, DNA damage and DNA repair

The most prominent changes in gene expression (Fig. 2, Table 4, Supplementary Tables 2 and 3) were found for genes involved in different steps of apoptosis, DNA damage, p53 function and DNA

Table 3 Inflammation and tissue injury in the cortices of cases selected for microarray analysis

	Multiple sclerosis ($n = 3$)	Tuberculous meningitis ($n = 3$)	Alzheimer's disease ($n = 3$)	Controls ($n = 3$)
T cells	91 (55)	541 (860)	11 (9)	11 (24)
Microglia/macrophages	757 (596)	2301 (1449)	552 (218)	544 (252)
Extent of demyelination	41 (23)	1 (1)	0 (0)	0 (0)
Oligodendrocytes	23 (14)$^{+}$/ 105 (52)$^{\#}$	50 (32)	82 (23)	67 (107)
Neurons	154 (70)$^{+}$/ 221 (60)$^{\#}$	214 (24)	198 (43)	235 (15)
Axonal spheroids	8 (93)$^{+}$/ 6 (30)$^{\#}$	3 (7)	8 (26)	0 (2)

This table summarizes the quantification of immunohistochemical results to determine the levels of inflammation, demyelination, and neurodegeneration in disease cases selected for microarray analysis. CD3-positive T cells, CD68-positive microglia/macrophages, TPPP/p25-positive oligodendrocytes, neurons and neurofilament-reactive dystrophic axons were counted (counts/mm^2). The extent of demyelination was calculated as demyelinated area in relation to total cortex area. Results are presented as median value and range (in brackets). + = lesion centre; # = lesion edge.

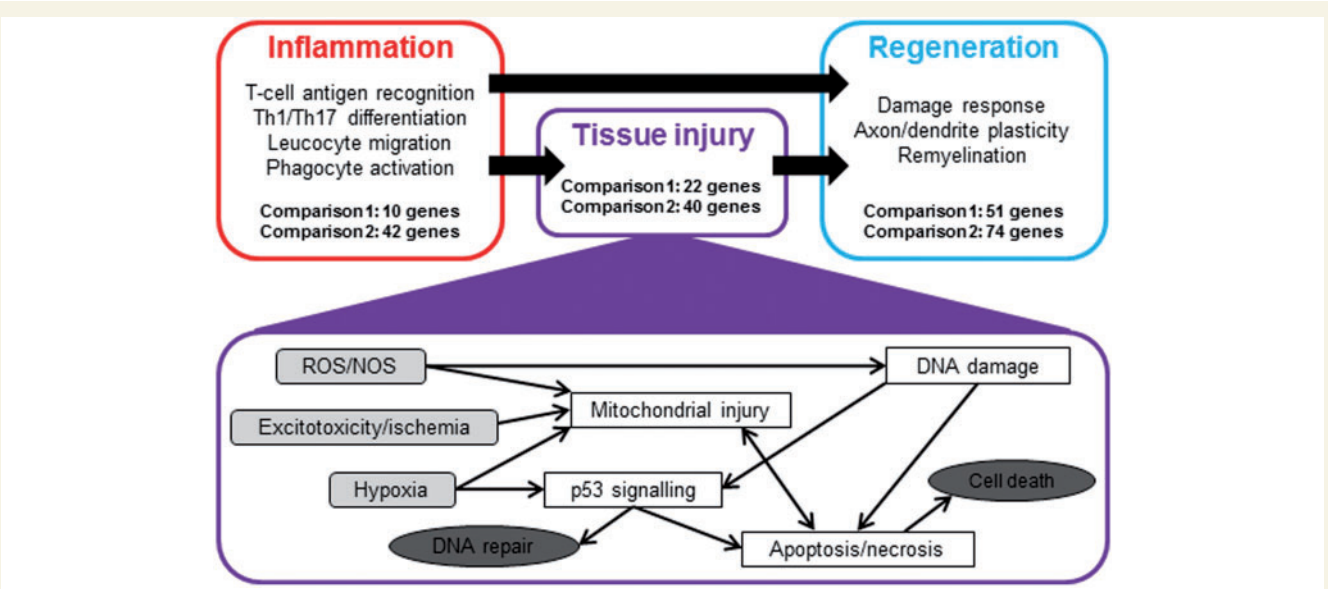

Figure 2 Based on their known functions, multiple sclerosis-specific genes can be grouped into three major categories. Summary of differentially expressed genes in multiple sclerosis lesions compared with tuberculous meningitis, Alzheimer's disease and control cortex. The genes are grouped according to their possible functions into inflammation-, tissue injury- and regeneration-related genes. Detailed lists of the differentially expressed genes are provided in Supplementary Tables 2 and 3. Potential molecular pathways of tissue injury are summarized in the lower half of the figure. The most important multiple sclerosis-specific genes concerning tissue injury and regeneration are listed in Tables 4 and 5. ROS/NOS = reactive oxygen species/nitric oxide synthase.

repair (Table 4). They also included potassium and chloride channels controlling cell volume in the course of cell body or cell process degeneration, or genes involved in the modulation of excitotoxic or ischaemic cell death. This was in line with the identification of another cluster of genes with multiple sclerosis-specific expression, which was related to hypoxia, oxidative stress and mitochondria (Table 4).

Category 3: reaction to tissue injury and association with tissue repair

This category constituted the largest one (Fig. 2, Table 5, Supplementary Tables 2 and 3). A major subgroup included genes coding for proteins involved in RNA metabolism or regulation of transcription or translation. Another considerable cluster was related to development in general and to brain development in particular. It comprised genes necessary for various cellular functions such as cell survival, growth, and differentiation or control of cytoskeletal components (in particular tubulin turnover). One further group contained genes functionally associated with axonal and synaptic biology and regeneration (Table 5). The majority of these were either involved in axonal growth and guidance, or in synapse function. As expected, we also found significantly increased expression of some myelin- and oligodendrocyte-related genes in multiple sclerosis. Their expression was highest in Cases MS2 and MS3, which contained demyelinated and remyelinating lesion centres with rims of active demyelination at the border to the white matter.

Table 4 Microarray analysis: most important genes regarding tissue injury

Gene symbol	Gene name (gene function)	Log_2	*P*-value
	Reactive oxygen species/nitric oxide synthase		
GGTLC1	Gamma-glutamyltransferase light chain 1 (glutathione metabolism)	5.70	
DDAH2	Dimethylarginine dimethylaminohydrolase 2 (NOS synthesis)	5.54	
TXNIP	Thioredoxin interacting protein (increases production of ROS)	4.76	
SMOX	Spermine oxidase (radical scavenger)	4.38	
GSTT1	Glutathione S-transferase theta 1 (antioxidant)	4.07	
OGDHL	Oxoglutarate dehydrogenase-like (oxidoreductase)	2.77	<0.001
ARHGEF18	Rho/rac guanine nucleotide exchange factor 18 (ROS production)	2.28	0.001
HP	Haptoglobin (cellular iron ion homeostasis)	2.01	0.005
ASPHD1	Aspartate beta-hydroxylase domain containing 1 (oxidoreductase)	1.48	0.001
NOS1AP	Nitric oxide synthase 1 adaptor protein (neuronal nitric oxide synthesis)	0.91	0.009
NAPRT1	Nicotinate phosphoribosyltransferase domain containing 1 (oxidative stress response)	0.88	0.005
	Excitotoxicity/ischaemia		
CLCA1	Chloride channel, calcium activated, family member 1 (NMDAR-induced ischemic cell death)	6.91	
SLC8A1	Solute carrier family 8 (sodium/calcium exchanger), member 1 (protective role in ischemia)	5.39	
ACMSD	Aminocarboxymuconate semialdehyde decarboxylase (may inhibit excitotoxicity)	−4.91	
CACNA1E	Calcium channel, voltage-dependent, R type, alpha 1E subunit (protective role in ischemia)	−5.13	
	Hypoxia		
OS9	Amplified in osteosarcoma (binds and inactivates HIF1α)	4.81	
CITED4	Cbp/p300-interacting transactivator, with Glu/Asp-rich carboxy-terminal domain, 4 (inhibits HIF1α signalling)	0.90	0.009
CITED2	Cbp/p300-interacting transactivator, with Glu/Asp-rich carboxy-terminal domain, 2 (negative regulator for HIF1α)	−4.54	
HSD11B2	Hydroxysteroid (11-beta) dehydrogenase 2 (response to hypoxia)	−4.55	
USP20	Ubiquitin specific peptidase 20 (deubiquitinates HIF1α)	−4.74	
	Mitochondrial injury		
SLC25A4	Solute carrier family 25 (mitochondrial carrier; adenine nucleotide translocator), member 4 (exchange of cytoplasmic ADP with mitochondrial ATP)	5.96	
PYCR1	Pyrroline-5-carboxylate reductase 1 (NADP+ generation)	5.31	
ND6	NADH-ubiquinone oxidoreductase chain 6 (mitochondrial respiratory chain)	5.07	
TSFM	Ts translation elongation factor, mitochondrial (translation of mitochondrial proteins)	2.04	0.006
	p53 signalling		
ZMIZ1	Zinc finger, MIZ-type containing 1 (coactivator of p53)	5.34	
RNF144B	Ring finger 144B (induces p53-dependent cell death)	4.77	
P2RX6	P2X purinoceptor 6 (p53 responsive gene)	4.30	
IGFBP7	Insulin-like growth factor binding protein 7 (p53 responsive gene)	4.21	
CUL9	p53-associated parkin-like cytoplasmic protein (regulation of p53 localization)	2.14	0.007
ZNHIT1	Zinc finger, HIT type 1 (induces p53-mediated apoptosis)	1.76	0.008
BRD7	Bromodomain containing 7 (p53 interactor)	1.43	0.005
MEG3	Maternally expressed 3 (p53 interactor)	0.97	0.009
PSRC1	Proline/serine-rich coiled-coil 1 (p53-regulated growth suppression)	−4.54	
ZNF668	Zinc finger protein 668 (p53 regulation)	−5.92	
DEC1	Deleted in esophageal cancer 1 (p53-dependent senescence)	−8.99	
	DNA damage		
DFFA	DNA fragmentation factor, 45 kDa, alpha polypeptide (DNA fragmentation during apoptosis)	−4.95	
	DNA repair		
RAD51	RAD51 homolog (repair of DNA double strand breaks)	6.06	
ERCC5	Excision repair cross-complementing rodent repair deficiency, complementation group 5 (nucleotide excision repair)	5.28	
LIG1	Ligase I, DNA, ATP-dependent (base excision repair and DNA replication)	0.98	0.009
WRNIP1	Werner helicase interacting protein 1 (initiation of DNA synthesis)	−4.87	
	Apoptosis		
BMF	Bcl2 modifying factor (proapoptotic)	7.53	
TMEM16G	Transmembrane protein 16G (may function during apoptotic cell death)	4.74	
PACS2	Phosphofurin acidic cluster sorting protein 2 (induces mitochondrial cytochrome C release)	4.69	

(continued)

Table 4 Continued

Gene symbol	Gene name (gene function)	Log_2	*P*-value
ASAH2	N-acylsphingosine amidohydrolase (non-lysosomal ceramidase) 2 (blocks ceramide-induced apoptosis)	4.68	
HRASLS3	HRAS-like suppressor 3 (involved in interferon-induced cell death)	4.00	
MAP3K10	Mitogen-activated protein kinase kinase kinase 10 (nerve growth factor- induced neuronal apoptosis)	3.28	0.001
TMEM16H	Transmembrane protein 16H (may function during apoptotic cell death)	2.70	<0.001
PRKCZ	Protein kinase C, zeta (Fas ligand-induced apoptosis)	2.55	0.004
TNFAIP1	Tumor necrosis factor, alpha-induced protein 1 (proapoptotic)	2.38	0.002
PKD1	Polycystic kidney disease 1 (proapoptotic)	2.11	0.004
TRADD	TNFRSF1A-associated via death domain (proapoptotic)	1.67	0.004
CMTM5	CKLF-like MARVEL transmembrane domain containing (induces apoptosis in synergy with TNFα)	1.52	<0.001
WISP1	WNT1 inducible signaling pathway protein 1 (attenuates apoptosis)	−5.94	

Genes of both microarray analysis approaches are included. For Comparison 1 [significantly ($P < 0.01$) changed genes in Cases MS1–3 in comparison with all other cases (Cases TB1–3, AD1–3 and CO1–3; $n = 9$)], log_2 fold-changes as well as the corresponding *P*-values are shown. For Comparison 2 [massively up- or downregulated genes (log_2 fold-changes >4 or <-4.5, respectively) in Case MS1 in comparison with all other cases], only the log_2-transformed fold-changes are given. A complete gene list is provided in Supplementary Tables 2 and 3. NOS = nitric oxide synthase; ROS = Reactive oxygen species.

Table 5 Microarray analysis: most important genes regarding the regeneration of neuronal processes

Gene symbol	Gene name (gene function)	Log_2	*P*-value
GPM6A	Glycoprotein M6A (neuronal differentiation; neurite outgrowth; neuronal plasticity)	6.10	
PHF10	PHD finger protein 10 (dendrite growth)	5.71	
CACNB2	Calcium channel, voltage-dependent, beta 2 subunit (axon guidance; synaptic transmission)	5.63	
TNN	Tenascin N (axon repulsion)	5.48	
NEO1	Neogenin homolog 1 (axon guidance)	4.12	
ANKS3	Ankyrin repeat and sterile alpha motif domain containing 3 (axon guidance)	4.03	
CARTPT	CART prepropeptide (neuronal development)	2.54	0.000
LRFN2	Leucine rich repeat and fibronectin type III domain containing 2 (dendrite outgrowth; synapse formation)	1.79	0.000
MYLK2	Myosin light chain kinase 2 (synaptic plasticity)	1.50	0.001
SLIT1	Slit homolog 1 (axon guidance)	1.47	0.003
SORL1	Sortilin-related receptor, L(DLR class) A repeats-containing (discussed for axon regeneration)	1.42	0.003
TRIM2	Tripartite motif-containing 2 (axon outgrowth)	1.25	0.003
STMN3	Stathmin-like 3 (neurite development)	1.23	0.009
ISLR2	Immunoglobulin superfamily containing leucine-rich repeat 2 (axon outgrowth)	0.94	0.007
CAMK2B	Calcium/calmodulin-dependent protein kinase (CaM kinase) II beta (plasticity of glutamatergic synapses)	−4.60	
ACTL6B	Actin-like 6B (neuronal development; dendrite morphogenesis)	−4.85	
SEMA6B	Sema domain, transmembrane domain (TM), and cytoplasmic domain, (semaphorin) 6B (axon guidance)	−5.39	

Genes of both microarray analysis approaches are included. For Comparison 1 [significantly ($P < 0.01$) changed genes in Cases MS1–3 in comparison with all other cases (TB1–3, AD1–3, and CO1–3; $n = 9$)], log_2 fold-changes as well as the corresponding *P*-values are shown. For Comparison 2 [massively up- or downregulated genes (log_2 fold-changes >4 or <-4.5, respectively) in MS1 in comparison with all other cases], only the log_2-transformed fold-changes are given. A complete gene list is provided in Supplementary Tables 2 and 3.

Increased oxidative damage and DNA strand breaks in cortical multiple sclerosis lesions compared with tuberculous meningitis and other controls

So far, our microarray data suggested multiple sclerosis-specific changes in the expression of genes related to oxidative injury and DNA damage in cortical lesions. We therefore attempted to confirm these data in the entire sample or cases with multiple sclerosis listed in Table 1. From the individual cases with multiple sclerosis, cortical lesions were selected, which contained a demyelinated area with oligodendrocyte loss, surrounded by an area of microglia activation with interspersed macrophages containing early tissue degradation products and an adjacent area of normal appearing grey matter. In comparison with control cortices, a significant loss of neurons (31.1% loss; $P < 0.01$) was seen in the demyelinated areas of multiple sclerosis cortex, which is in the range of that described previously (Vercellino *et al*., 2005; Wegner

et al., 2006; Magliozzi *et al*., 2010; Choi *et al*., 2012) and in the cortices of Alzheimer's disease (40%; $P < 0.001$; Supplementary Fig. 2). Our previous studies of active white matter lesions (Haider *et al*., 2011; Fischer *et al*., 2012) indicated that immunohistochemistry for oxidized phospholipids (E06 immunoreactivity) is a sensitive marker for degenerating oligodendrocytes and dystrophic axons. In cortical multiple sclerosis lesions, we observed a similar immunoreactivity for oxidized phospholipids in the mentioned cell types, concentrated at sites of ongoing demyelination (Fig. 3A and M). Neurons with intense cytoplasmic accumulation of oxidized phospholipids (Fig. 3N) were significantly more abundant in active cortical multiple sclerosis lesions than in lesions of tuberculous meningitis, luetic meningitis, chronic purulent meningitis ($P < 0.05$), Alzheimer's disease ($P < 0.05$) or controls ($P < 0.001$; Figs 3A–D and 4A). In addition, oxidatively damaged neurons showed process fragmentation (Fig. 3E–H, O and P) or nuclear changes of necrosis- or apoptosis-like cell death as defined earlier (Muller *et al*., 2004) (Fig. 3I and J). Furthermore, nerve cells exhibiting central chromatolysis, a sign of proximal axon transection, also showed profound E06 immunoreactivity (Fig. 3K and L). Additionally, we performed TUNEL staining for DNA strand breaks. TUNEL-positive nuclei of neurons and oligodendrocytes were most frequently seen in multiple sclerosis lesions in the areas of active demyelination and tissue injury (Fig. 3R), whereas their number was much smaller in the demyelinated lesion centre and the normal appearing grey matter (Fig. 4B). Few TUNEL-positive nuclei were seen in the cortex of controls or patients with tuberculous meningitis (Figs 3S and 4B). Double staining for TUNEL and oxidized phospholipids showed that neurons with oxidative damage either contained condensed nuclei with high TUNEL reactivity, suggestive for apoptosis (Fig. 3U), or nuclei with small focal spots of damaged DNA (Fig. 3T). Immunohistochemistry for activated caspase 3 was negative throughout the whole tissue sample, suggesting caspase-independent cell death (data not shown). Apoptosis inducing factor was present in the mitochondria of healthy neurons in control and multiple sclerosis tissue (Fig 3V). In active multiple sclerosis lesions, however, neurons were seen, which in addition to mitochondrially located apoptosis inducing factor also showed diffuse apoptosis inducing factor immunoreactivity in the cytoplasm and presence of apoptosis inducing factor in cell nuclei (Fig. 3W).

Cells with cytoplasmic accumulation of oxidized phospholipids were mainly present in cortical areas with high density of activated microglia expressing the NADPH oxidase component p22phox (Fig. 5A). Processes of p22phox-positive microglia were attached either to the cell body (Fig. 5B) or to dendrites of neurons with oxidative injury (Fig. 5C). Immunohistochemistry for inducible nitric oxide synthase (iNOS) revealed that active cortical multiple sclerosis lesions contain only few inducible nitric oxide synthase-reactive cell bodies or processes of microglia (Fig. 5D). Macrophages with high inducible nitric oxide synthase immunoreactivity were seen in more advanced white matter lesions (Fig. 5E). These findings are in line with our microarray results showing an up-regulation of certain NADPH oxidase subunits (mainly components of NOX1 and NOX2 complexes) in cortical multiple sclerosis lesions in comparison with tuberculous meningitis or control cases (Fig. 5F).

Discussion

Active cortical demyelination and neurodegeneration in multiple sclerosis are associated with inflammation in the cortical tissue itself (Lucchinetti *et al*., 2011) or in the meninges (Kutzelnigg *et al*., 2005; Howell *et al*., 2011). It has thus been suggested that tissue injury is either mediated by inflammatory cells or their soluble mediators diffusing into the cortex and inducing tissue damage either directly or indirectly through microglia activation (Howell *et al*., 2011). Several types of inflammatory cells, including T cells or B cells, are regarded as particularly important in multiple sclerosis pathogenesis and thought to trigger demyelination and neurodegeneration in a non-specific 'bystander' fashion (Wisniewski and Bloom, 1975). A previous study (Moll *et al*., 2008) indicated that cortical demyelination may be multiple sclerosis-specific, but this conclusion was based on diseases with inflammatory reactions quite different from multiple sclerosis. In our study, we confirm this view by focusing on diseases, which to our knowledge more closely reflect key inflammatory components operating in multiple sclerosis lesions. Thus, demyelination and neurodegeneration in multiple sclerosis are not unspecific consequences of inflammation, but appear to involve multiple sclerosis-specific mechanisms of tissue injury.

Microarray studies have been performed on cortical tissue of multiple sclerosis before. They revealed changes related to mitochondrial function in the non-demyelinated motor cortex (Dutta *et al*., 2006), to axonal transport and synaptic function (Dutta *et al*., 2011), to the regulation of oligodendrocyte differentiation (Schmidt *et al*., 2012) and to intrathecal immunoglobulin synthesis (Torkildsen *et al*., 2010). In contrast to our current study, they focused on normal appearing grey matter or demyelinated areas, but not on areas of active demyelination and tissue injury. Furthermore, they did not include other disease controls. Thus, the prominent expression of immunoglobulin related genes described by Torkildsen *et al*., (2010) did not appear in our results, because tuberculous meningitis, similar to multiple sclerosis, shows profound intrathecal immunoglobulin synthesis.

Our results showed multiple sclerosis-specific gene expression changes in mainly three different molecular pathways: inflammation, oxidative stress associated with DNA damage, and regenerative mechanisms affecting oligodendrocytes, neurons and neuronal cell processes.

Multiple sclerosis-specific gene expression related to inflammation (Supplementary Tables 2 and 3) involved molecules important for antigen presentation and polarization of MHC class I and II restricted T cells towards Th1 and Th17 pathways (Tzartos *et al*., 2008) or macrophage/microglia activation. Downregulation of the expression of the co-stimulatory molecule CTLA4 in active cortical lesions (Supplementary Table 3) is in agreement with the proposed anti-inflammatory function of this molecule in patients with multiple sclerosis (Joller *et al*., 2012). Results supporting our current data have been reported before in other gene expression studies (Whitney *et al*., 1999; Lock *et al*., 2002; Mycko *et al*., 2003) and interpretation of the data is in agreement with inflammatory pathways identified in genome-wide association studies on multiple sclerosis susceptibility (Sawcer *et al*., 2011). Our study further

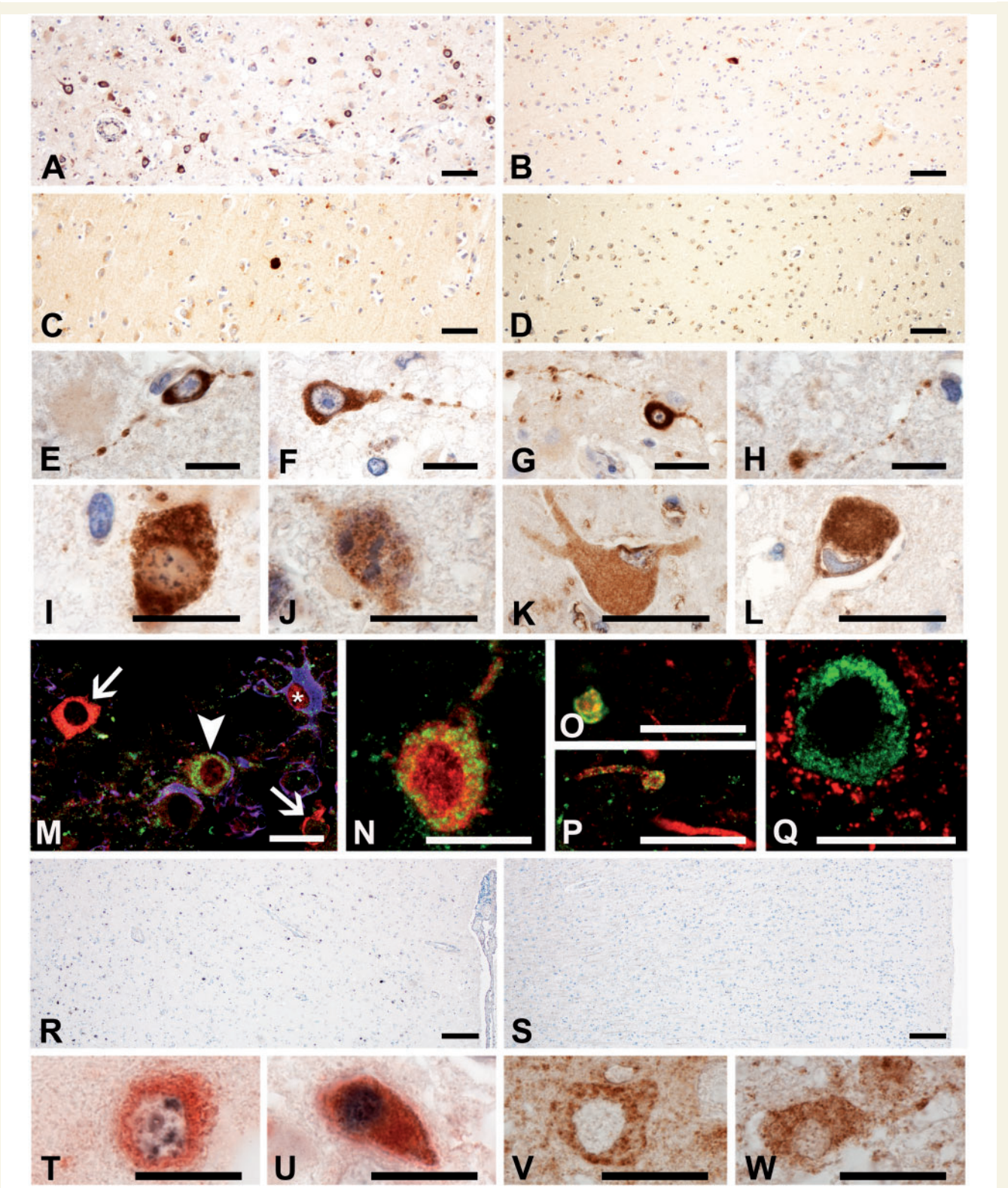

Figure 3 Cytoplasmic accumulation of oxidized phospholipids (E06 reactivity) in cortical multiple sclerosis lesions. (**A–D**) Cortical tissue from multiple sclerosis (**A**; MS1), tuberculous meningitis (**B**; TB2), and Alzheimer's disease (**C**; AD2) patients and control (**D**; CO3) cases. Numerous cells with strong cytoplasmic E06 immunoreactivity are seen in the multiple sclerosis cortex (**A**), while only sparse E06-positive cells are seen in the other conditions (**B–D**). However, some granular, lipofuscin-like E06 immunoreactivity is visible mainly within neurons and macrophages in all examined cases. (**E–H**) Neurons with extensive cytoplasmic accumulation of oxidized phospholipids show beading and fragmentation of their processes in active cortical multiple sclerosis lesions. (**I** and **J**) Patterns of degeneration (Muller *et al*., 2004) in neurons with extensive accumulation of oxidized phospholipids. Neurons with numerous fine speckles of condensed chromatin resembling

(continued)

identified a number of molecules that are instrumental in leucocyte trafficking into inflammatory lesions including integrin alpha 9, a binding partner of vascular cell adhesion molecule (VCAM). Blockade of VCAM/integrin interaction is currently a very effective anti-inflammatory treatment in patients with multiple sclerosis (Polman *et al*., 2006). Our results also indicate that selectins, which mediate inflammation in peripheral organs and the brain through integrin activation (Prendergast and Anderton, 2009; Alvarez *et al*., 2011; Zarbock *et al*., 2012), may play a role in regulating leucocyte trafficking in cortical multiple sclerosis lesions in the progressive stage of the disease. High expression of some selectins has also been shown before in microarray studies on microdissected blood vessels from patients with multiple sclerosis (Cunnea *et al*., 2010).

Regarding mechanisms of tissue injury, which were in the main focus of our study, our results suggest that oxidative damage plays a major role in the processes of cortical oligodendrocyte degeneration, demyelination and neuronal damage. These resemble mechanisms observed previously in active white matter lesions and adjacent normal appearing white matter. Expression of enzymes involved in oxygen (Gray *et al*., 2008; Fischer *et al*., 2012) and nitric oxide radical production (Liu *et al*., 2001; Marik *et al*., 2007; Zeis *et al*., 2009), the abundance of oxidized lipids and DNA in degenerating oligodendrocytes and axons (Haider *et al*., 2011), the increased expression of molecules involved in antioxidant defence (van Horssen *et al*., 2008) and the presence of hypoxia-like tissue injury in active lesions and the adjacent normal appearing white matter (Aboul-Enein *et al*., 2003; Graumann *et al*., 2003; Trapp and Stys, 2009) have been shown before. Oxidative stress is assumed to lead to mitochondrial injury in multiple sclerosis lesions (Dutta *et al*., 2006; Mahad *et al*., 2008; Campbell *et al*., 2011; Lassmann *et al*., 2012). Here we show that immunoreactivity for oxidized phospholipids is much higher in neurons of active cortical multiple sclerosis lesions than in all other conditions studied (tuberculous meningitis, Alzheimer's disease, and control subjects). Furthermore, the expression of genes involved in DNA damage and repair was highly up-regulated in multiple sclerosis lesions in comparison with other inflammatory or neurodegenerative controls such as tuberculous meningitis or Alzheimer's disease (Table 4, Supplementary Tables 2 and 3). This was also confirmed by the much higher incidence of cells with TUNEL reactivity in areas of active demyelination and tissue injury. TUNEL reactivity, which has been shown before to occur in low incidence in inactive cortical multiple sclerosis lesions (Peterson *et al*., 2001), may reflect apoptotic cell death, but also reversible DNA injury. In line with previous studies, apoptosis in multiple sclerosis lesions was not associated with caspase 3 activation (Barnett and Prineas, 2004), but with the liberation of apoptosis inducing factor from mitochondria and its nuclear translocation (Veto *et al*., 2010). Neuronal cell death within active lesion areas may at least in part be responsible for neuronal loss in established lesions.

The mechanisms that drive oxidative injury and neurodegeneration in multiple sclerosis lesions are currently not fully understood. Persistent inflammation in meninges and cortical parenchyma appears to be one important driving force (Howell *et al*., 2011; Choi *et al*., 2012; Lucchinetti *et al*., 2011). In addition, factors related to ageing and to chronicity of the disease may play a role. As an example, age-related iron accumulation in the human brain may amplify oxidative injury (Lassmann *et al*., 2012). Furthermore, it was shown in a recent study that the topography of cortical lesions may be related to distant lesions within the white or deep grey matter (Kolasinski *et al*., 2012), indicating a role of anterograde or retrograde degeneration in the precipitation of cortical lesions. This may also in part explain the differences between cortical lesions in multiple sclerosis and tuberculous meningitis, the latter exposing the cortex to inflammation in the absence of pre-existing distant neurodegeneration.

An interesting observation of our study is that oxidative injury of neurons in the multiple sclerosis cortex coincides with beading and fragmentation of axons and dendrites. Degeneration of neuronal processes was present in cells, in which the peri-nuclear cell body remained morphologically intact. This is further supported by our microarray analyses comprising many genes related to axonal, dendritic, and synaptic regeneration. A similar result has been obtained in previous work analysing gene expression in hippocampal multiple sclerosis lesions (Dutta *et al*., 2011), and it was suggested that the profound axonal injury in cortical multiple sclerosis lesions is related to increased vulnerability of demyelinated axons

Figure 3 Continued
'necrosis-like' cell death (**I**) as well as neurons with large fragments of condensed chromatin resembling 'apoptosis-like' cell death (**J**) can be found. (**K** and **L**) Neurons with central chromatolysis as a reaction to proximal axonal transsection show intense reactivity for oxidized phospholipids. (**M**) E06 reactivity in oligodendrocytes in active cortical multiple sclerosis lesion of Case MS1. The figure shows two normal oligodendrocytes (white arrows), one oligodendrocyte with accumulation of oxidized phospholipids (white arrowhead) and an astrocyte (white asterisk). Triple antibody labeling for E06 (green), carboanhydrase (red), and glial fibrillary acidic protein (blue). (**N**) Calbindin-positive nerve cell in a cortical multiple sclerosis lesion with cytoplasmic E06 immunoreactivity. Double antibody labelling for E06 (green) and calbindin (red). (**O** and **P**) Double staining for E06 (green) and neurofilament (red) shows individual dystrophic axons with E06 immunoreactivity. (**Q**) Double staining for E06 (green) and synaptophysin (red) shows a neuron with oxidized phospholipids, but no E06 immunoreactivity in synaptophysin-positive synapses.(**R**) Cortical lesion of Case MS1 stained for DNA strand breaks with TUNEL (black nuclei); the number of nuclei with DNA strand breaks is similar to the number of cells stained for oxidized phospholipids, shown in **A**. (**S**) TUNEL staining of control cortex (CO3); no nuclear TUNEL reactivity is seen. (**T** and **U**) Double staining for TUNEL (black) and E06 (red) shows either spotted TUNEL reactivity in E06 positive neurons with otherwise intact nuclei (**T**) or intense TUNEL reactivity in neurons with condensed apoptotic like nuclei (**U**). (**V** and **W**) Apoptosis inducing factor immunoreactivity is present in a staining pattern resembling mitochondria in normal neurons (**V**), but in addition shows diffuse cytoplasmic staining and nuclear reactivity in neurons with beaded cell processes (**W**). Scale bars: **A–D** = 100 μm; **E–Q** and **T–W** = 50 μm; **R** and **S** = 200 μm.

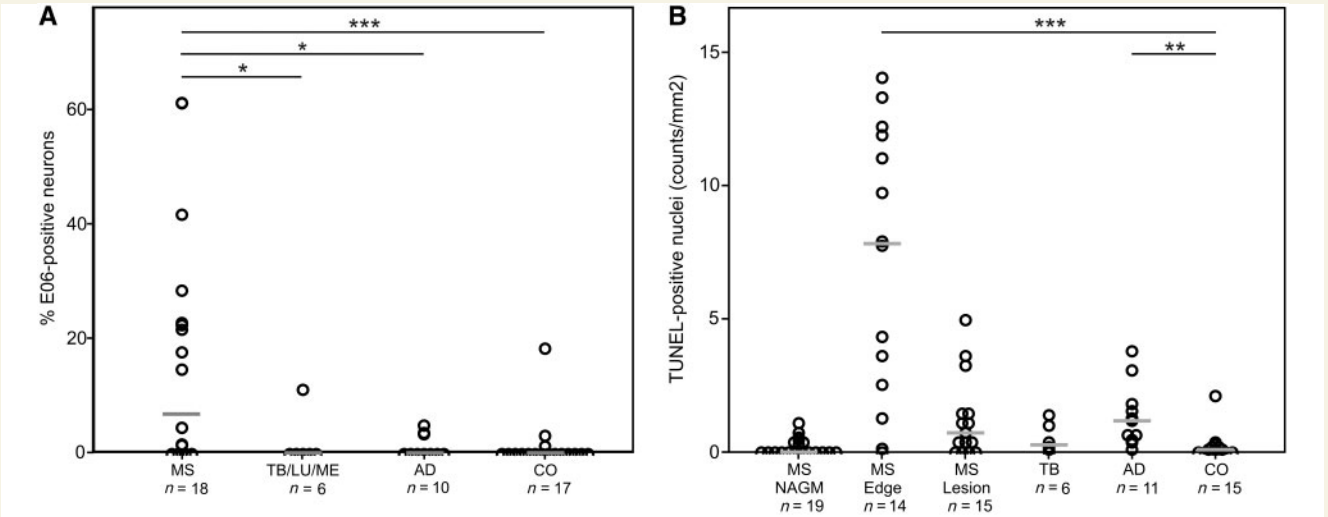

Figure 4 Neurons with intense cytoplasmic accumulation of oxidized phospholipids and DNA strand breaks are abundant in active cortical multiple sclerosis lesions. (**A**) Scatter plot displaying the percentage of neurons with intense, cytoplasmic E06 immunoreactivity in relation to the total number of counted cortical neurons. In active multiple sclerosis lesion areas, significantly more oxidatively damaged neurons are present in comparison with other inflammatory diseases (tuberculous meningitis/luetic meningitis/chronic purulent meningitis; $P < 0.05$), neurodegenerative diseases (Alzheimer's disease; $P < 0.05$), or control cases ($P < 0.001$). The median value for each group is indicated by a grey bar. (**B**) Scatter plot of TUNEL-positive nuclei in the cortex of patients with multiple sclerosis in comparison with that of tuberculous meningitis, Alzheimer's disease and control subjects. Cells with DNA strand breaks are mainly present in the area of lesional activity in patients with multiple sclerosis (multiple sclerosis edge). NAGM = normal appearing grey matter; MS = multiple sclerosis; TB = tuberculous meningitis; LM = luetic meningitis; ME = chronic purulent meningitis; AD = Alzheimer's disease; CO = control; $*P < 0.05$; $***P < 0.001$.

(Dutta *et al*., 2011). Our study proposes an additional mechanism: direct oxidative injury and focal damage of axons and dendrites due to the primary destructive events. Partial repair of neuronal cell processes in cortical multiple sclerosis lesions may occur in parallel with remyelination (Albert *et al*., 2007) and may be associated with functional plasticity seen in MRI studies (Rocca and Filippi, 2007; Caramia *et al*., 2010).

We are aware that our study has limitations regarding the analysis of whole-genome microarrays. RNA was isolated from formaldehyde-fixed and paraffin-embedded material, which is known to be inferior in comparison with fresh frozen tissue. Eisele *et al*. (2012) published a comprehensive study comparing formaldehyde-fixed and paraffin-embedded to fresh frozen material using, among others, tissue derived from our archives. Eisele *et al*. (2012) showed that although integrity measurements of RNA isolated from formaldehyde-fixed and paraffin-embedded material resulted in very low integrity numbers, amplicons with a length of <150 bp were still detectable. Eisele *et al*. (2012) performed quantitative PCR-based transcript profiling analysing the expression of 84 extracellular matrix-related genes and identified a transcript loss of 47% in formaldehyde-fixed and paraffin-embedded-derived samples in comparison with fresh frozen material. Of course, such false negative results can be expected in our study as well. We tried to minimize this problem accordingly by first of all using only tissue blocks that showed reasonable RNA preservation, as evidenced by strong *in situ* hybridization signals after a short time of development. Secondly, stringent RNA quality criteria were applied to ensure that only samples with sufficiently long RNA fragments were further processed. Thirdly, we used whole-genome microarrays from Agilent. As shown in Supplementary Table 4, most of the probes of Agilent arrays were located within the last exon. Because the RNA fragments contained in our samples were amplified using poly(A) tail primers, the binding probability to the corresponding microarray probes was maximized. Fourthly, we focused on either highly significantly changed genes ($P < 0.01$) or used restrictive cut-offs ($\log_2$ fold-changes >4 or <-4.5). Additionally, we did not focus on single gene analysis, which would require much more stringent molecular and biochemical confirmation of the identified molecules. Instead, we used the microarray data for the identification of interconnected pathways within specific and extremely well characterized lesions. The involvement of these pathways in multiple sclerosis pathology, but not necessarily the involvement of single pathway-revealing molecules, was then evaluated in immunohistochemical analyses using a much larger sample of cases and lesions. We want to point out that our microarray analyses also included a single case comparison (Case MS1 in comparison with all other cases). This was done, since this case showed an extreme degree of cortical inflammatory demyelinating activity, which is extremely rare in multiple sclerosis tissue available for pathological analysis (Kutzelnigg *et al*., 2005; Lucchinetti *et al*., 2011) and for this reason may be particularly informative with respect to the questions addressed in this study. Despite these limitations, a strong argument for the validity of our data is the fact that $>80\%$ of

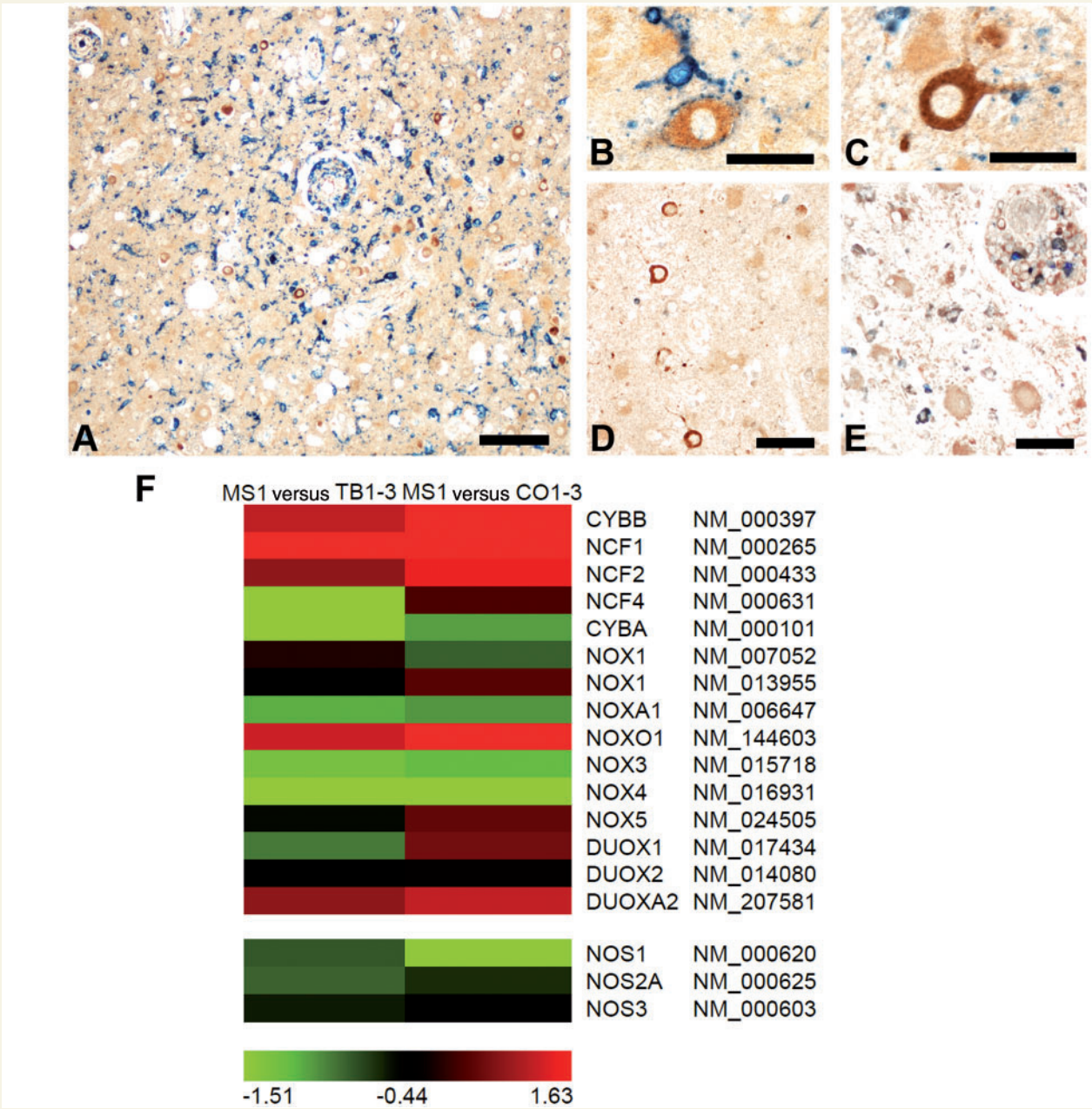

Figure 5 Oxidative damage in cortical multiple sclerosis lesions is mainly driven by NADPH oxidases. (**A–C**) Cells containing oxidized phospholipids (brown) are located in areas with numerous microglia expressing the NADPH oxidase component p22phox (blue). P22phox-positive, activated microglia embrace oxidatively damaged neurons with their processes (**B**) or are in contact with neuronal cell processes (**C**). (**D** and **E**) Double labelling for E06 (brown) and inducible nitric oxide synthase (iNOS; blue). Cortical multiple sclerosis lesions with profound cellular accumulation of oxidized phospholipids contain only few microglia cells or processes reactive for inducible nitric oxide synthase (**D**). In contrast, macrophages with high immunoreactivity for inducible nitric oxide synthase are seen in more advanced lesions in the white matter of the same section (**E**). (**F**) The heat map presents colour-coded $\log_2$-transformed fold-changes of genes coding for NADPH oxidase components or nitric oxide synthase enzymes. For this analysis, the fulminate Case MS1 was compared with either tuberculous meningitis (TB1–3; *left* column) or controls (CO1–3; *right* column). The comparisons are in line with immunohistochemical studies suggesting oxidative damage to be driven by NOX1 and NOX2 components of NADPH oxidases and not by nitric oxide synthaseenzymes. The colour gradient was computed using 10th, 50th, and 90th percentiles. Green, black and red colours indicate downregulated, unchanged, and upregulated genes, respectively. The official gene symbol and RefSeq annotation number are shown for each gene. MS = multiple sclerosis; TB = tuberculous meningitis; CO = control; Scale bars: **A** = 200 μm; **B** and **C** = 50 μm; **D** and **E** = 100 μm.

gene expression changes identified by our approach are related to interconnected molecular pathways, which in part have been suggested to operate in multiple sclerosis lesions before.

In conclusion, our study shows that focal plaque-like demyelination is a specific feature of cortical multiple sclerosis lesions and is associated with excessive oxidative damage, mainly affecting oligodendrocytes, neurons and their cell processes. The reason for excessive oxidative injury remains currently unresolved and may be related to the nature of the inflammatory process or to factors determining the susceptibility of neuronal tissue to inflammation in multiple sclerosis, such as brain ageing or accumulation of pre-existing damage. To answer this question, more extensive studies are necessary concentrating on highly active and inflammatory cortical multiple sclerosis lesions, which are very rare in archival autopsy material, but are sometimes seen in biopsies of multiple sclerosis brain tissue obtained during the early stages of the disease (Lucchinetti *et al*., 2011).

Acknowledgements

We thank Ulrike Köck, Angela Kury and Marianne Leisser for excellent technical assistance.

Funding

This study was funded by the PhD programme Cell Communication in Health and Disease (CCHD, co-funded by the Austrian Science Fund (Project W 1205 and the Medical University Vienna) and by the Austrian Science Fund (FWF, Project P24245-B19 to HL).

Supplementary material

Supplementary material is available at *Brain* online.

References

Aboul-Enein F, Rauschka H, Kornek B, Stadelmann C, Stefferl A, Bruck W, et al. Preferential loss of myelin-associated glycoprotein reflects hypoxia-like white matter damage in stroke and inflammatory brain diseases. J Neuropath Exp Neurol 2003; 62: 25–33.

Albert M, Antel J, Bruck W, Stadelmann C. Extensive cortical remyelination in patients with chronic multiple sclerosis. Brain Pathol 2007; 17: 129–38.

Alvarez JI, Cayrol R, Prat A. Disruption of central nervous system barriers in multiple sclerosis. Biochim Biophys Acta 2011; 1812: 252–64.

Barnett MH, Prineas JW. Relapsing and remitting multiple sclerosis: pathology of the newly forming lesion. Ann Neurol 2004; 55: 458–68.

Bauer J, Elger CE, Hans VH, Schramm J, Urbach H, Lassmann H, et al. Astrocytes are a specific immunological target in Rasmussen's encephalitis. Ann Neurol 2007; 62: 67–80.

Bian W, Harter K, Hammond-Rosenbluth KE, Lupo JM, Kelley DA, Vigneron DB, et al. A serial in vivo 7T magnetic resonance phase imaging study of white matter lesions in multiple sclerosis. Mult Scler 2012; 19: 69–75.

Bien CG, Bauer J, Deckwerth TL, Wiendl H, Deckert M, Wiestler OD, et al. Destruction of neurons by cytotoxic T cells: a new pathogenic mechanism in Rasmussen's encephalitis. Ann Neurol 2002; 51: 311–18.

Bo L, Vedeler CA, Nyland HI, Trapp BD, Mork SJ. Subpial demyelination in the cerebral cortex of multiple sclerosis patients. J Neuropathol Exp Neurol 2003; 62: 723–32.

Breitschopf H, Suchanek G, Gould RM, Colman DR, Lassmann H. In situ hybridization with digoxigenin-labeled probes: sensitive and reliable detection method applied to myelinating rat brain. Acta Neuropathol 1992; 84: 581–7.

Campbell GR, Ziabreva I, Reeve AK, Krishnan KJ, Reynolds R, Howell O, et al. Mitochondrial DNA deletions and neurodegeneration in multiple sclerosis. Ann Neurol 2011; 69: 481–92.

Caramia F, Tinelli E, Francia A, Pozzilli C. Cognitive deficits in multiple sclerosis: a review of functional MRI studies. Neurol Sci 2010; 31: S239–43.

Choi S, Howell OW, Carassiti D, Magliozzi R, Gveric D, Muraro PA, et al. Meningeal inflammation plays a role in the pathology of primary progressive multiple sclerosis. Brain 2012; 135: 2925–37.

Cunnea P, McMahon J, O'Connell E, Mashayekhi K, Fitzgerald U, McQuaid S. Gene expression analysis of the microvascular compartment in multiple sclerosis using laser microdissected blood vessels. Acta Neuropathol 2010; 119: 601–15.

Dutta R, Chang A, Doud MK, Kidd GJ, Ribaudo MV, Young EA, et al. Demyelination causes synaptic alterations in hippocampi from multiple sclerosis patients. Ann Neurol 2011; 69: 445–54.

Dutta R, McDonough J, Yin X, Peterson J, Chang A, Torres T, et al. Mitochondrial dysfunction as a cause of axonal degeneration in multiple sclerosis patients. Ann Neurol 2006; 59: 478–89.

Dutta R, Trapp BD. Mechanisms of neuronal dysfunction and degeneration in multiple sclerosis. Prog Neurobiol 2011; 93: 1–12.

Eisele S, Krumbholz M, Fischer MT, Mohan H, Junker A, Arzberger T, et al. Prospects of transcript profiling for mRNAs and microRNAs using formalin fixed paraffin embedded dissected autoptic multiple sclerosis lesions. Brain Pathol 2012; 22: 607–12.

Fischer MT, Sharma R, Lim JL, Haider L, Frischer JM, Drexhage J, et al. NADPH oxidase expression in active multiple sclerosis lesions in relation to oxidative tissue damage and mitochondrial injury. Brain 2012; 135: 886–99.

Geurts JJ, Bo L, Roosendaal SD, Hazes T, Daniels R, Barkhof F, et al. Extensive hippocampal demyelination in multiple sclerosis. J Neuropathol Exp Neurol 2007; 66: 819–27.

Gold R, Schmied M, Rothe G, Zischler H, Breitschopf H, Wekerle H, et al. Detection of DNA-fragmentation in apoptosis: application of in situ nick translation to cell culture systems and tissue sections. J Histochem Cytochem 1993; 41: 1023–30.

Graumann U, Reynolds R, Steck AJ, Schaeren-Wiemers N. Molecular changes in normal appearing white matter in multiple sclerosis are characteristic of neuroprotective mechanisms against hypoxic insult. Brain Pathol 2003; 13: 554–73.

Gray E, Thomas TL, Betmouni S, Scolding N, Love S. Elevated activity and microglial expression of myeloperoxidase in demyelinated cerebral cortex in multiple sclerosis. Brain Pathol 2008; 18: 86–95.

Haider L, Fischer MT, Frischer JM, Bauer J, Hoftberger R, Botond G, et al. Oxidative damage in multiple sclerosis lesions. Brain 2011; 134: 1914–24.

Hoftberger R, Fink S, Aboul-Enein F, Botond G, Olah J, Berki T, et al. Tubulin polymerization promoting protein (TPPP/p25) as a marker for oligodendroglial changes in multiple sclerosis. Glia 2010; 58: 1847–57.

Howell OW, Reeves CA, Nicholas R, Carassiti D, Radotra B, Gentleman SM, et al. Meningeal inflammation is widespread and linked to cortical pathology in multiple sclerosis. Brain 2011; 134: 2755–71.

Joller N, Peters A, Anderson AC, Kuchroo VK. Immune checkpoints in central nervous system autoimmunity. Immunol Rev 2012; 248: 122–39.

King G, Payne S, Walker F, Murray GI. A highly sensitive detection method for immunohistochemistry using biotinylated tyramine. J Pathol 1997; 183: 237–41.

Kolasinski J, Stagg CJ, Chance SA, DeLuca GC, Esiri MM, Chang EH, et al. A combined post-mortem MRI and quantitative histological study of multiple sclerosis pathology. Brain 2012; 135: 2938–51.

Kutzelnigg A, Faber-Rod JC, Bauer J, Lucchinetti CF, Sorensen PS, Laursen H, et al. Widespread demyelination in the cerebellar cortex in multiple sclerosis. Brain Pathol 2007; 17: 38–44.

Kutzelnigg A, Lucchinetti CF, Stadelmann C, Bruck W, Rauschka H, Bergmann M, et al. Cortical demyelination and diffuse white matter injury in multiple sclerosis. Brain 2005; 128: 2705–12.

Lassmann H, Bancher C, Breitschopf H, Wegiel J, Bobinski M, Jellinger K, et al. Cell death in Alzheimer's disease evaluated by DNA-fragmentation in situ. Acta Neuropathol 1995; 89: 35–41.

Lassmann H, Bruck W, Lucchinetti CF. The immunopathology of multiple sclerosis: an overview. Brain Pathol 2007; 17: 210–18.

Lassmann H, van Horssen J, Mahad D. Progressive multiple sclerosis: pathology and pathogenesis. Nat Rev Neurol 2012; 8: 647–56.

Liu JS, Zhao ML, Brosnan CF, Lee SC. Expression of inducible nitric oxide synthase and nitrotyrosine in multiple sclerosis lesions. Am J Pathol 2001; 158: 2057–66.

Lock C, Hermans G, Pedotti R, Brendolan A, Schadt E, Garren H, et al. Gene-microarray analysis of multiple sclerosis lesions yields new targets validated in autoimmune encephalomyelitis. Nat Med 2002; 8: 500–8.

Lucchinetti CF, Popescu BF, Bunyan RF, Moll NM, Roemer SF, Lassmann H, et al. Inflammatory cortical demyelination in early multiple sclerosis. N Engl J Med 2011; 365: 2188–97.

Mahad D, Ziabreva I, Lassmann H, Turnbull D. Mitochondrial defects in acute multiple sclerosis lesions. Brain 2008; 131: 1722–35.

Magliozzi R, Howell OW, Reeves C, Roncaroli F, Nicholas R, Serafini B, et al. A gradient of neuronal loss and meningeal inflammation in multiple sclerosis. Ann Neurol 2010; 68: 477–93.

Marik C, Felts PA, Bauer J, Lassmann H, Smith KJ. Lesion genesis in a subset of patients with multiple sclerosis: a role for innate immunity? Brain 2007; 130: 2800–15.

Mitew S, Kirkcaldie MT, Halliday GM, Shepherd CE, Vickers JC, Dickson TC. Focal demyelination in Alzheimer's disease and transgenic mouse models. Acta Neuropathol 2010; 119: 567–77.

Moll NM, Rietsch AM, Ransohoff AJ, Cossoy MB, Huang D, Eichler FS, et al. Cortical demyelination in PML and MS: Similarities and differences. Neurology 2008; 70: 336–43.

Muller GJ, Stadelmann C, Bastholm L, Elling F, Lassmann H, Johansen FF. Ischemia leads to apoptosis–and necrosis-like neuron death in the ischemic rat hippocampus. Brain Pathol 2004; 14: 415–24.

Mycko MP, Papoian R, Boschert U, Raine CS, Selmaj KW. cDNA microarray analysis in multiple sclerosis lesions: detection of genes associated with disease activity. Brain 2003; 126: 1048–57.

Palinski W, Horkko S, Miller E, Steinbrecher UP, Powell HC, Curtiss LK, et al. Cloning of monoclonal autoantibodies to epitopes of oxidized lipoproteins from apolipoprotein E-deficient mice. Demonstration of epitopes of oxidized low density lipoprotein in human plasma. J Clin Invest 1996; 98: 800–14.

Peterson JW, Bo L, Mork S, Chang A, Trapp BD. Transected neurites, apoptotic neurons, and reduced inflammation in cortical multiple sclerosis lesions. Ann Neurol 2001; 50: 389–400.

Piddlesden SJ, Lassmann H, Zimprich F, Morgan BP, Linington C. The demyelinating potential of antibodies to myelin oligodendrocyte glycoprotein is related to their ability to fix complement. Am J Pathol 1993; 143: 555–64.

Polman CH, O'Connor PW, Havrdova E, Hutchinson M, Kappos L, Miller DH, et al. A randomized, placebo-controlled trial of natalizumab for relapsing multiple sclerosis. N Engl J Med 2006; 354: 899–910.

Prendergast CT, Anderton SM. Immune cell entry to central nervous system–current understanding and prospective therapeutic targets. Endocr Metab Immune Disord Drug Targets 2009; 9: 315–27.

Rocca MA, Filippi M. Functional MRI in multiple sclerosis. J Neuroimaging 2007; 17 (Suppl 1): 36S–41S.

Sawcer S, Hellenthal G, Pirinen M, Spencer CC, Patsopoulos NA, Moutsianas L, et al. Genetic risk and a primary role for cell-mediated immune mechanisms in multiple sclerosis. Nature 2011; 476: 214–19.

Schmidt F, van den Eijnden M, Pescini Gobert R, Saborio GP, Carboni S, Alliod C, et al. Identification of VHY/Dusp15 as a regulator of oligodendrocyte differentiation through systematic genomics approach. PLoS One 2012; 7: e40457.

Stam NJ, Vroom TM, Peters PJ, Pastoors EB, Ploegh HL. HLA-A- and HLA-B-specific monoclonal antibodies reactive with free heavy chains in western blots, in formalin-fixed, paraffin-embedded tissue sections and in cryo-immuno-electron microscopy. Int Immunol 1990; 2: 113–25.

Torkildsen O, Stansberg C, Angelskar SM, Kooi EJ, Geurts JJ, van der Valk P, et al. Upregulation of immunoglobulin-related genes in cortical sections from multiple sclerosis patients. Brain Pathol 2010; 20: 720–9.

Trapp BD, Stys PK. Virtual hypoxia and chronic necrosis of demyelinated axons in multiple sclerosis. Lancet Neurol 2009; 8: 280–91.

Tzartos JS, Friese MA, Craner MJ, Palace J, Newcombe J, Esiri MM, et al. Interleukin-17 production in central nervous system-infiltrating T cells and glial cells is associated with active disease in multiple sclerosis. Am J Pathol 2008; 172: 146–55.

van Horssen J, Schreibelt G, Drexhage J, Hazes T, Dijkstra CD, van der Valk P, et al. Severe oxidative damage in multiple sclerosis lesions coincides with enhanced antioxidant enzyme expression. Free Radic Biol Med 2008; 45: 1729–37.

Vercellino M, Plano F, Votta B, Mutani R, Giordana MT, Cavalla P. Grey matter pathology in multiple sclerosis. J Neuropath Exp Neurol 2005; 64: 1101–7.

Veto S, Acs P, Bauer JK, Lassmann H, Berente Z, Setalo G Jr, et al. Inhibiting poly(ADP-ribose) polymerase: a potential therapy against oligodendrocyte death. Brain 2010; 133: 822–34.

Wegner C, Esiri MM, Chance SA, Palace J, Matthews PM. Neocortical neuronal, synaptic, and glial loss in multiple sclerosis. Neurology 2006; 67: 960–7.

Whitney LW, Becker KG, Tresser NJ, Caballero-Ramos CI, Munson PJ, Prabhu VV, et al. Analysis of gene expression in mutiple sclerosis lesions using cDNA microarrays. Ann Neurol 1999; 46: 425–8.

Wisniewski HM, Bloom BR. Primary demyelination as a nonspecific consequence of a cell-mediated immune reaction. J Exp Med 1975; 141: 346–59.

Zarbock A, Kempf T, Wollert KC, Vestweber D. Leukocyte integrin activation and deactivation: novel mechanisms of balancing inflammation. J Mol Med (Berl) 2012; 90: 353–9.

Zeis T, Probst A, Steck AJ, Stadelmann C, Bruck W, Schaeren-Wiemers N. Molecular changes in white matter adjacent to an active demyelinating lesion in early multiple sclerosis. Brain Pathol 2009; 19: 459–66.